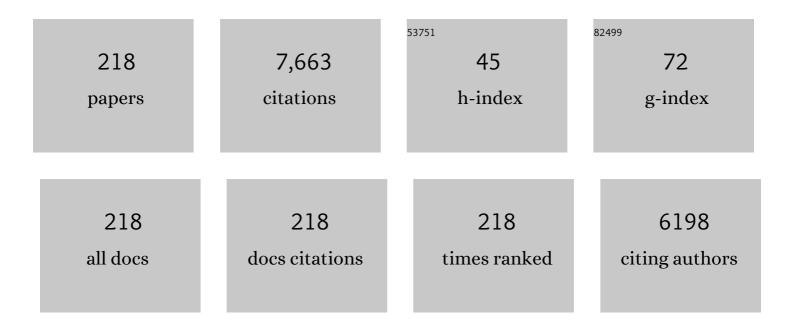
Shaoxian Song

List of Publications by Year in descending order

Source: https://exaly.com/author-pdf/1090652/publications.pdf Version: 2024-02-01



#	Article	IF	CITATIONS
1	Methylene blue removal from water using the hydrogel beads of poly(vinyl alcohol)-sodium alginate-chitosan-montmorillonite. Carbohydrate Polymers, 2018, 198, 518-528.	5.1	299
2	Geopolymerization reaction, microstructure and simulation of metakaolin-based geopolymers at extended Si/Al ratios. Cement and Concrete Composites, 2017, 79, 45-52.	4.6	266
3	Removal of methylene blue from water with montmorillonite nanosheets/chitosan hydrogels as adsorbent. Applied Surface Science, 2018, 448, 203-211.	3.1	208
4	Self-assembled gels of Fe-chitosan/montmorillonite nanosheets: Dye degradation by the synergistic effect of adsorption and photo-Fenton reaction. Chemical Engineering Journal, 2020, 379, 122322.	6.6	202
5	Efficient Ofloxacin degradation with Co(â¡)-doped MoS2 nano-flowers as PMS activator under visible-light irradiation. Chemical Engineering Journal, 2020, 401, 125978.	6.6	186
6	Two-Dimensional Molybdenum Disulfide as a Superb Adsorbent for Removing Hg ²⁺ from Water. ACS Sustainable Chemistry and Engineering, 2017, 5, 7410-7419.	3.2	167
7	Removal of heavy metals and dyes by clay-based adsorbents: From natural clays to 1D and 2D nano-composites. Chemical Engineering Journal, 2021, 420, 127574.	6.6	144
8	Eco-friendly geopolymer prepared from solid wastes: A critical review. Chemosphere, 2021, 267, 128900.	4.2	134
9	Synthesis of Fluorinated Graphene/CoAl-Layered Double Hydroxide Composites as Electrode Materials for Supercapacitors. ACS Applied Materials & Interfaces, 2017, 9, 5204-5212.	4.0	125
10	Comparison of Pb(II) adsorption onto graphene oxide prepared from natural graphites: Diagramming the Pb(II) adsorption sites. Applied Surface Science, 2016, 364, 620-627.	3.1	114
11	AFM study on the adsorption of Hg ²⁺ on natural molybdenum disulfide in aqueous solutions. Physical Chemistry Chemical Physics, 2017, 19, 3837-3844.	1.3	107
12	Oxidation of Molybdenum Disulfide Sheet in Water under in Situ Atomic Force Microscopy Observation. Journal of Physical Chemistry C, 2017, 121, 9938-9943.	1.5	102
13	A novel core-shell structural montmorillonite nanosheets/stearic acid composite PCM for great promotion of thermal energy storage properties. Solar Energy Materials and Solar Cells, 2019, 192, 57-64.	3.0	91
14	Effects of curing temperature on the compressive strength and microstructure of copper tailing-based geopolymers. Chemosphere, 2020, 253, 126754.	4.2	91
15	Recent advances in structural engineering of molybdenum disulfide for electrocatalytic hydrogen evolution reaction. Chemical Engineering Journal, 2021, 405, 127013.	6.6	91
16	Combination formation in the reinforcement of metakaolin geopolymers with quartz sand. Cement and Concrete Composites, 2017, 80, 115-122.	4.6	88
17	High-performance two-dimensional montmorillonite supported-poly(acrylamide-co-acrylic acid) hydrogel for dye removal. Environmental Pollution, 2020, 257, 113574.	3.7	86
18	Design of 3D-network montmorillonite nanosheet/stearic acid shape-stabilized phase change materials for solar energy storage. Solar Energy Materials and Solar Cells, 2020, 204, 110233.	3.0	78

#	Article	IF	CITATIONS
19	Enhanced removal of methyl orange on exfoliated montmorillonite/chitosan gel in presence of methylene blue. Chemosphere, 2020, 238, 124693.	4.2	77
20	Defect-rich molybdenum disulfide as electrode for enhanced capacitive deionization from water. Desalination, 2018, 446, 21-30.	4.0	76
21	Adsorption of heavy metals on molybdenum disulfide in water: A critical review. Journal of Molecular Liquids, 2019, 292, 111390.	2.3	72
22	Pb(ΙΙ) removal from water using porous hydrogel of chitosan-2D montmorillonite. International Journal of Biological Macromolecules, 2019, 128, 85-93.	3.6	70
23	Controllable incorporation of oxygen in MoS2 for efficient adsorption of Hg2+ in aqueous solutions. Journal of Hazardous Materials, 2020, 384, 121382.	6.5	70
24	Effects of oxidation on the defect of reduced graphene oxides in graphene preparation. Journal of Colloid and Interface Science, 2015, 450, 68-73.	5.0	68
25	Reexamining calcination of kaolinite for the synthesis of metakaolin geopolymers - roles of dehydroxylation and recrystallization. Journal of Non-Crystalline Solids, 2017, 460, 74-80.	1.5	68
26	Preparation of Montmorillonite Nanosheets through Freezing/Thawing and Ultrasonic Exfoliation. Langmuir, 2019, 35, 2368-2374.	1.6	68
27	Degradation of fluoroquinolones in homogeneous and heterogeneous photo-Fenton processes: A review. Chemosphere, 2021, 270, 129481.	4.2	68
28	Adsorption of As(V) inside the pores of porous hematite in water. Journal of Hazardous Materials, 2016, 307, 312-317.	6.5	66
29	Two-dimensional molybdenum disulfide as adsorbent for high-efficient Pb(II) removal from water. Applied Materials Today, 2017, 9, 220-228.	2.3	66
30	Enhancement of cadmium adsorption by EPS-montmorillonite composites. Environmental Pollution, 2019, 252, 1509-1518.	3.7	65
31	In Situ Reduction of Au(I) for Efficient Recovery of Gold from Thiosulfate Solution by the 3D MoS ₂ /Chitosan Aerogel. ACS Sustainable Chemistry and Engineering, 2020, 8, 3673-3680.	3.2	62
32	MoS2@sponge with double layer structure for high-efficiency solar desalination. Desalination, 2020, 481, 114359.	4.0	62
33	Synthesis of carboxymethyl cellulose-chitosan-montmorillonite nanosheets composite hydrogel for dye effluent remediation. International Journal of Biological Macromolecules, 2020, 165, 1-10.	3.6	61
34	Effect of Cu2+ and Fe3+ on the depression of molybdenite in flotation. Minerals Engineering, 2019, 130, 101-109.	1.8	59
35	Facile Preparation of Three-Dimensional MoS ₂ Aerogels for Highly Efficient Solar Desalination. ACS Applied Materials & Interfaces, 2020, 12, 32673-32680.	4.0	57
36	Synthesis of chitosan cross-linked 3D network-structured hydrogel for methylene blue removal. International Journal of Biological Macromolecules, 2019, 141, 98-107.	3.6	55

#	Article	IF	CITATIONS
37	Viscosities of Binary and Ternary Mixtures of Water, Alcohol, Acetone, and Hexane. Journal of Dispersion Science and Technology, 2008, 29, 1367-1372.	1.3	54
38	Removal of Cd (II) from water by using nano-scale molybdenum disulphide sheets as adsorbents. Journal of Molecular Liquids, 2018, 263, 526-533.	2.3	53
39	Emerging Hexagonal Mo ₂ C Nanosheet with (002) Facet Exposure and Cu Incorporation for Peroxymonosulfate Activation Toward Antibiotic Degradation. ACS Applied Materials & Interfaces, 2021, 13, 14342-14354.	4.0	53
40	Mussel-inspired Fe3O4@Polydopamine(PDA)-MoS2 core–shell nanosphere as a promising adsorbent for removal of Pb2+ from water. Journal of Molecular Liquids, 2019, 282, 598-605.	2.3	52
41	Combined Electrosorption and Chemisorption of As(V) in Water by Using Fe-rGO@AC Electrode. ACS Sustainable Chemistry and Engineering, 2017, 5, 6532-6538.	3.2	50
42	Correlation of montmorillonite exfoliation with interlayer cations in the preparation of two-dimensional nanosheets. RSC Advances, 2017, 7, 41471-41478.	1.7	49
43	A novel method for determining the thickness of hydration shells on nanosheets: A case of montmorillonite in water. Powder Technology, 2017, 306, 74-79.	2.1	49
44	Three-dimensional montmorillonite/Ag nanowire aerogel supported stearic acid as composite phase change materials for superior solar-thermal energy harvesting and storage. Composites Science and Technology, 2022, 217, 109121.	3.8	49
45	Thermal Modification of the Molybdenum Disulfide Surface for Tremendous Improvement of Hg ²⁺ Adsorption from Aqueous Solution. ACS Sustainable Chemistry and Engineering, 2018, 6, 9065-9073.	3.2	48
46	Electrosorption of fluoride on TiO2-loaded activated carbon in water. Colloids and Surfaces A: Physicochemical and Engineering Aspects, 2016, 502, 66-73.	2.3	47
47	Competition of Hg2+ adsorption and surface oxidation on MoS2 surface as affected by sulfur vacancy defects. Applied Surface Science, 2019, 483, 521-528.	3.1	47
48	Electrophoretic mobility study for heterocoagulation of montmorillonite with fluorite in aqueous solutions. Powder Technology, 2017, 309, 61-67.	2.1	46
49	Immobilization of mercury using high-phosphate culture-modified microalgae. Environmental Pollution, 2019, 254, 112966.	3.7	46
50	A Robust Molecular Catalyst Generated Inâ€Situ for Photo―and Electrochemical Water Oxidation. ChemSusChem, 2017, 10, 862-875.	3.6	43
51	Preparation of ion-imprinted montmorillonite nanosheets/chitosan gel beads for selective recovery of Cu(â¡) from wastewater. Chemosphere, 2020, 252, 126560.	4.2	43
52	Precise Cation Recognition in Two-Dimensional Nanofluidic Channels of Clay Membranes Imparted from Intrinsic Selectivity of Clays. ACS Nano, 2022, 16, 4930-4939.	7.3	43
53	DESALINATION BY CAPACITIVE DEIONIZATION WITH CARBON-BASED MATERIALS AS ELECTRODE: A REVIEW. Surface Review and Letters, 2013, 20, 1330003.	0.5	42
54	Simultaneous Sorption of Arsenate and Fluoride on Calcined Mg–Fe–La Hydrotalcite-Like Compound from Water. ACS Sustainable Chemistry and Engineering, 2018, 6, 16287-16297.	3.2	42

#	Article	IF	CITATIONS
55	Immobilization forms of ZnO in the solidification/stabilization (S/S) of a zinc mine tailing through geopolymerization. Journal of Materials Research and Technology, 2019, 8, 5728-5735.	2.6	42
56	Simultaneous removal of Hg2+, Pb2+ and Cd2+ from aqueous solutions on multifunctional MoS2. Journal of Molecular Liquids, 2019, 296, 111987.	2.3	42
57	Hydrophilic MoS2/polydopamine (PDA) nanocomposites as the electrode for enhanced capacitive deionization. Separation and Purification Technology, 2020, 236, 116298.	3.9	42
58	Adsorption of As(III) on porous hematite synthesized from goethite concentrate. Chemosphere, 2017, 169, 188-193.	4.2	41
59	Selective flotation of fluorite from barite using trisodium phosphate as a depressant. Minerals Engineering, 2019, 134, 390-393.	1.8	41
60	Effect of anions species on copper removal from wastewater by using mechanically activated calcium carbonate. Chemosphere, 2019, 230, 127-135.	4.2	40
61	Effects of Aluminum Dosage on Gel Formation and Heavy Metal Immobilization in Alkali-Activated Municipal Solid Waste Incineration Fly Ash. Energy & Fuels, 2020, 34, 4727-4733.	2.5	40
62	Reduction mechanism of Au metal ions into Au nanoparticles on molybdenum disulfide. Nanoscale, 2019, 11, 9488-9497.	2.8	39
63	Flexible 2D@3D Janus evaporators for high-performance and continuous solar desalination. Desalination, 2022, 525, 115483.	4.0	39
64	Recovery of [Au(CN) 2] â^' from gold cyanidation with graphene oxide as adsorbent. Separation and Purification Technology, 2017, 186, 63-69.	3.9	38
65	Chemical forms of lead immobilization in alkali-activated binders based on mine tailings. Cement and Concrete Composites, 2018, 92, 198-204.	4.6	38
66	Consolidation of mine tailings through geopolymerization at ambient temperature. Journal of the American Ceramic Society, 2019, 102, 2451-2461.	1.9	38
67	Synthesis of unique-morphological hollow microspheres of MoS2@montmorillonite nanosheets for the enhancement of photocatalytic activity and cycle stability. Journal of Materials Science and Technology, 2020, 41, 88-97.	5.6	38
68	Effects of aluminum on the expansion and microstructure of alkali-activated MSWI fly ash-based pastes. Chemosphere, 2020, 240, 124986.	4.2	38
69	Molecular dynamics simulations of hydration shell on montmorillonite (001) in water. Surface and Interface Analysis, 2016, 48, 976-980.	0.8	37
70	Cometabolic biodegradation of antibiotics by ammonia oxidizing microorganisms during wastewater treatment processes. Journal of Environmental Management, 2022, 305, 114336.	3.8	37
71	Characterisation of reduced graphene oxides prepared from natural flaky, lump and amorphous graphites. Materials Research Bulletin, 2016, 78, 119-127.	2.7	36
72	Solidification of municipal solid waste incineration fly ash and immobilization of heavy metals using waste glass in alkaline activation system. Chemosphere, 2021, 283, 131240.	4.2	36

#	Article	IF	CITATIONS
73	Effective harvesting of microalgae by coagulation–flotation. Royal Society Open Science, 2017, 4, 170867.	1.1	35
74	Algal biomass from the stable growth phase as a potential biosorbent for Pb(<scp>ii</scp>) removal from water. RSC Advances, 2017, 7, 34600-34608.	1.7	35
75	Piezo-Photocatalytic Reduction of Au(I) by Defect-Rich MoS ₂ Nanoflowers for Efficient Gold Recovery from a Thiosulfate Solution. ACS Sustainable Chemistry and Engineering, 2021, 9, 589-598. Adsorption of the complex ion Au <mml:math <="" td="" xmlns:mml="http://www.w3.org/1998/Math/MathML"><td>3.2</td><td>34</td></mml:math>	3.2	34
76	altimg="si1.gif" overflow="scroll"> <mml:mrow><mml:mo stretchy="false">(<mml:mtext>CN</mml:mtext><mml:msubsup><mml:mrow><mml:mo) etqqc<br="" tj="">sulfur-impregnated activated carbon in aqueous solutions. Journal of Colloid and Interface Science,</mml:mo)></mml:mrow></mml:msubsup></mml:mo </mml:mrow>	0 0 0 rgBT /(Dverlgck 10 T
77	2010, 349, 602-606. Geothermal clay-based geopolymer binders: Synthesis and microstructural characterization. Applied Clay Science, 2017, 146, 223-229.	2.6	33
78	EXFOLIATION AND CHARACTERIZATION OF LAYERED SILICATE MINERALS: A REVIEW. Surface Review and Letters, 2014, 21, 1430001.	0.5	32
79	Cell surface characterization of some oleaginous green algae. Journal of Applied Phycology, 2016, 28, 2323-2332.	1.5	32
80	Co-disposal of MSWI fly ash and spent caustic through alkaline-activation: Immobilization of heavy metals and organics. Cement and Concrete Composites, 2020, 114, 103824.	4.6	32
81	Adsorption toward Cu(II) and inhibitory effect on bacterial growth occurring on molybdenum disulfide-montmorillonite hydrogel surface. Chemosphere, 2020, 248, 126025.	4.2	32
82	Construction of MoS2 nano-heterojunction via ZnS doping for enhancing in-situ photocatalytic reduction of gold thiosulfate complex. Chemical Engineering Journal, 2020, 394, 124866.	6.6	32
83	High temperature enhances lipid accumulation in nitrogen-deprived Scenedesmus obtusus XJ-15. Journal of Applied Phycology, 2016, 28, 831-837.	1.5	31
84	Microscale control of edge defect and oxidation on molybdenum disulfide through thermal treatment in air and nitrogen atmospheres. Applied Surface Science, 2018, 462, 471-479.	3.1	31
85	Design of MtNS/SA microencapsulated phase change materials for enhancement of thermal energy storage performances: Effect of shell thickness. Solar Energy Materials and Solar Cells, 2019, 200, 109935.	3.0	31
86	Molybdenum disulfide/montmorillonite composite as a highly efficient adsorbent for mercury removal from wastewater. Applied Clay Science, 2020, 184, 105370.	2.6	31
87	Novel rapid room temperature synthesis of conjugated microporous polymer for metal-free photocatalytic degradation of fluoroquinolones. Journal of Hazardous Materials, 2020, 398, 122928.	6.5	31
88	Adsorption of AsV in aqueous solutions on porous hematite prepared by thermal modification of a siderite - goethite concentrate. Environmental Chemistry, 2012, 9, 512.	0.7	30
89	Reducing the Entrainment of Gangue Fines in Low Grade Microcrystalline Graphite Ore Flotation Using Multi-Stage Grinding-Flotation Process. Minerals (Basel, Switzerland), 2017, 7, 38.	0.8	30
90	Role of Montmorillonite, Kaolinite, or Illite in Pyrite Flotation: Differences in Clay Behavior Based on Their Structures. Langmuir, 2020, 36, 10860-10867.	1.6	30

#	Article	IF	CITATIONS
91	Fundamental Studies of SHMP in Reducing Negative Effects of Divalent Ions on Molybdenite Flotation. Minerals (Basel, Switzerland), 2018, 8, 404.	0.8	29
92	Correlation of exfoliation performance with interlayer cations of montmorillonite in the preparation of twoâ€dimensional nanosheets. Journal of the American Ceramic Society, 2019, 102, 3908-3922.	1.9	29
93	Co-disposal of MSWI fly ash and spent caustic through alkaline-activation consolidation. Cement and Concrete Composites, 2021, 116, 103888.	4.6	29
94	Synergetic degradation of Methylene Blue through photocatalysis and Fenton reaction on two-dimensional molybdenite-Fe. Journal of Environmental Sciences, 2022, 111, 11-23.	3.2	29
95	Combined electrosorption and chemisorption of low concentration Pb(II) from aqueous solutions with molybdenum disulfide as electrode. Applied Surface Science, 2018, 455, 258-266.	3.1	28
96	Magnetic MoS2 nanosheets as recyclable solar-absorbers for high-performance solar steam generation. Renewable Energy, 2021, 163, 146-153.	4.3	28
97	Reusing warm-paste waste as catalyst for peroxymonosulfate activation toward antibiotics degradation under high salinity condition: Performance and mechanism study. Chemical Engineering Journal, 2021, 426, 131295.	6.6	28
98	Preparation of monolayer muscovite through exfoliation of natural muscovite. RSC Advances, 2015, 5, 52882-52887.	1.7	27
99	Preparation and characterization of self-assembly hydrogels with exfoliated montmorillonite nanosheets and chitosan. Nanotechnology, 2018, 29, 025605.	1.3	27
100	Using van der Waals heterostructures based on two-dimensional InSe–XS ₂ (X = Mo, W) as promising photocatalysts for hydrogen production. Journal of Materials Chemistry C, 2020, 8, 12509-12515.	2.7	27
101	Self-assembly montmorillonite nanosheets supported hierarchical MoS2 as enhanced catalyst toward methyl orange degradation. Materials Chemistry and Physics, 2020, 246, 122829.	2.0	27
102	Synchronous photosensitized degradation of methyl orange and methylene blue in water by visible-light irradiation. Journal of Molecular Liquids, 2021, 334, 116159.	2.3	27
103	Selection of microalgae for biodiesel production in a scalable outdoor photobioreactor in north China. Bioresource Technology, 2014, 174, 274-280.	4.8	26
104	Adsorption of fluoride at the interface of water with calcined magnesium–ferri–lanthanum hydrotalcite-like compound. RSC Advances, 2017, 7, 26104-26112.	1.7	26
105	Molecular Dynamics Study of Crystalline Swelling of Montmorillonite as Affected by Interlayer Cation Hydration. Jom, 2018, 70, 479-484.	0.9	26
106	Electrosorption of Pb(<scp>ii</scp>) in water using graphene oxide-bearing nickel foam as the electrodes. RSC Advances, 2017, 7, 23543-23549.	1.7	25
107	Vertical porous MoS2/hectorite double-layered aerogel as superior salt resistant and highly efficient solar steam generators. Renewable Energy, 2022, 194, 68-79.	4.3	25
108	Effect of layer charges on exfoliation of montmorillonite in aqueous solutions. Colloids and Surfaces A: Physicochemical and Engineering Aspects, 2018, 548, 92-97.	2.3	24

#	Article	IF	CITATIONS
109	The Influencing Mechanisms of Sodium Hexametaphosphate on Chalcopyrite Flotation in the Presence of MgCl2 and CaCl2. Minerals (Basel, Switzerland), 2018, 8, 150.	0.8	24
110	Preparation and characterization of flowerlike Al-doped Ni(OH)2 for supercapacitor applications. Chemical Physics, 2019, 521, 55-60.	0.9	24
111	Selective recovery of heavy metals from wastewater by mechanically activated calcium carbonate: Inspiration from nature. Chemosphere, 2020, 246, 125842.	4.2	24
112	Ion modification of transition cobalt oxide by soaking strategy for enhanced water splitting. Chemical Engineering Journal, 2021, 423, 130218.	6.6	24
113	Effects of aggregates on the mechanical properties and microstructure of geothermal metakaolin-based geopolymers. Results in Physics, 2018, 11, 267-273.	2.0	23
114	In-situ reduction of gold thiosulfate complex on molybdenum disulfide nanosheets for a highly-efficient recovery of gold from thiosulfate solutions. Hydrometallurgy, 2020, 195, 105369.	1.8	23
115	NiCoS <i>_x</i> @Cobalt Carbonate Hydroxide Obtained by Surface Sulfurization for Efficient and Stable Hydrogen Evolution at Large Current Densities. ACS Applied Materials & Interfaces, 2021, 13, 35647-35656.	4.0	23
116	Recent advances in engineering cobalt carbonate hydroxide for enhanced alkaline water splitting. Journal of Alloys and Compounds, 2021, 887, 161405.	2.8	23
117	Recyclable Fe3O4@Polydopamine (PDA) nanofluids for highly efficient solar evaporation. Green Energy and Environment, 2022, 7, 35-42.	4.7	22
118	Insights into the degradation mechanisms and pathways of cephalexin during homogeneous and heterogeneous photo-Fenton processes. Chemosphere, 2021, 285, 131417.	4.2	22
119	Co-influence of the pore size of adsorbents and the structure of adsorbates on adsorption of dyes. Desalination and Water Treatment, 2016, 57, 14686-14695.	1.0	21
120	Correlation of electrophoretic mobility with exfoliation of montmorillonite platelets in aqueous solutions. Colloids and Surfaces A: Physicochemical and Engineering Aspects, 2017, 525, 1-6.	2.3	21
121	The Influence of Common Chlorides on the Adsorption of SBX on Chalcopyrite Surface during Flotation Process. Mineral Processing and Extractive Metallurgy Review, 2019, 40, 129-140.	2.6	21
122	Utilization of carbonate-based tailings to remove Pb(II) from wastewater through mechanical activation. Science of the Total Environment, 2020, 698, 134270.	3.9	21
123	Salt coagulation or flocculation? In situ zeta potential study on ion correlation and slime coating with the presence of clay: A case of coal slurry aggregation. Environmental Research, 2020, 189, 109875.	3.7	21
124	Montmorillonite facilitated Pb(II) biomineralization by Chlorella sorokiniana FK in soil. Journal of Hazardous Materials, 2022, 423, 127007.	6.5	21
125	Preparation of microscale zero-valent iron-fly ash-bentonite composite and evaluation of its adsorption performance of crystal violet and methylene blue dyes. Environmental Science and Pollution Research, 2017, 24, 20050-20062.	2.7	20
126	Insight the effect of crystallinity of natural graphite on the electrochemical performance of reduced graphene oxide. Results in Physics, 2018, 11, 131-137.	2.0	19

#	Article	IF	CITATIONS
127	Correlation of Montmorillonite Sheet Thickness and Flame Retardant Behavior of a Chitosan–Montmorillonite Nanosheet Membrane Assembled on Flexible Polyurethane Foam. Polymers, 2019, 11, 213.	2.0	19
128	Three-dimensional reduced graphene oxide/montmorillonite nanosheet aerogels as electrode material for supercapacitor application. Applied Clay Science, 2021, 206, 106022.	2.6	19
129	Self-assembly hierarchical binary gel based on MXene and montmorillonite nanosheets for efficient and stable solar steam generation. Journal of Cleaner Production, 2022, 357, 132000.	4.6	19
130	Increasing the Fine Flaky Graphite Recovery in Flotation via a Combined MultipleTreatments Technique of Middlings. Minerals (Basel, Switzerland), 2017, 7, 208.	0.8	18
131	Novel approach to control adsorbent aggregation: iron fixed bentonite-fly ash for Lead (Pb) and Cadmium (Cd) removal from aqueous media. Frontiers of Environmental Science and Engineering, 2018, 12, 1.	3.3	18
132	The fundamental roles of monovalent and divalent cations with sulfates on molybdenite flotation in the absence of flotation reagents. RSC Advances, 2018, 8, 23364-23371.	1.7	18
133	Model-based assessment of estrogen removal by nitrifying activated sludge. Chemosphere, 2018, 197, 430-437.	4.2	17
134	Removal of Pb(<scp>ii</scp>) and Cr(<scp>vi</scp>) from aqueous solutions using the prepared porous adsorbent-supported Fe/Ni nanoparticles. RSC Advances, 2018, 8, 32063-32072.	1.7	17
135	Vanadium Transitions during Roasting-Leaching Process of Vanadium Extraction from Stone Coal. Minerals (Basel, Switzerland), 2018, 8, 63.	0.8	17
136	Synergistic effect in the reduction of Cr(VI) with Ag-MoS2 as photocatalyst. Applied Materials Today, 2020, 18, 100453.	2.3	17
137	Use of posnjakite containing sludge as catalyst for decoloring dye via photo-Fenton-like process. Journal of Cleaner Production, 2021, 293, 126184.	4.6	17
138	Efficient Recovery of Gold(I) from Thiosulfate Solutions through Photocatalytic Reduction with Mn(II)-Doped MoS ₂ . ACS Sustainable Chemistry and Engineering, 2021, 9, 11681-11690.	3.2	17
139	Double-layered montmorillonite/MoS2 aerogel with vertical channel for efficient and stable solar interfacial desalination. Applied Clay Science, 2022, 217, 106389.	2.6	17
140	Effect of interlayer cations on exfoliating 2D montmorillonite nanosheets with high aspect ratio: From experiment to molecular calculation. Ceramics International, 2019, 45, 17054-17063.	2.3	16
141	Oxygen-incorporated molybdenum disulfide nanosheets as electrode for enhanced capacitive deionization. Desalination, 2020, 496, 114758.	4.0	16
142	Multi-edged molybdenite achieved by thermal modification for enhancing Pb(II) adsorption in aqueous solutions. Chemosphere, 2020, 251, 126369.	4.2	16
143	Development of superior stable two-dimensional montmorillonite nanosheet based working nanofluids for direct solar energy harvesting and utilization. Applied Clay Science, 2021, 200, 105886.	2.6	16
144	Optimization of Supercritical CO ₂ Extraction of Essential Oil from <i>Artemisia annua</i> L. by Means of Response Surface Methodology. Journal of Essential Oil-bearing Plants: JEOP, 2017, 20, 314-327.	0.7	15

#	Article	IF	CITATIONS
145	Effect of droplet size of the emulsified kerosene on the floatation of amorphous graphite. Journal of Dispersion Science and Technology, 2017, 38, 889-894.	1.3	15
146	Correlation of aspect ratio of montmorillonite nanosheets with the colloidal properties in aqueous solutions. Results in Physics, 2019, 15, 102526.	2.0	15
147	Air Dispersion and Bubble Characteristics in a Downflow Flotation Column. Mineral Processing and Extractive Metallurgy Review, 2019, 40, 224-229.	2.6	15
148	As(V) removal from water using the La(III)- Montmorillonite hydrogel beads. Reactive and Functional Polymers, 2020, 147, 104456.	2.0	15
149	Efficient removal of As(V) from diluted aqueous solutions by Fe/La oxide magnetic microspheres. Journal of Cleaner Production, 2020, 273, 123134.	4.6	15
150	Regulation of coal flotation by the cations in the presence of clay. Fuel, 2020, 271, 117590.	3.4	15
151	Improvement of compressive strength of lime mortar with carboxymethyl cellulose. Journal of Materials Science, 2016, 51, 9279-9286.	1.7	14
152	Heterotrophic denitrifiers growing on soluble microbial products contribute to nitrous oxide production in anammox biofilm: Model evaluation. Journal of Environmental Management, 2019, 242, 309-314.	3.8	14
153	Effect of cristobalite on the mechanical behaviour of metakaolin-based geopolymer in artificial seawater. Advances in Applied Ceramics, 2020, 119, 29-36.	0.6	14
154	Synergistic performance of a sub-nanoscopic cobalt and imidazole grafted porous organic polymer for CO ₂ fixation to cyclic carbonates under ambient pressure without a co-catalyst. Journal of Materials Chemistry A, 2020, 8, 13916-13920.	5.2	14
155	STUDY ON DECOMPOSITION OF GOETHITE/SIDERITE IN THERMAL MODIFICATION THROUGH XRD, SEM AND TGA MEASUREMENTS. Surface Review and Letters, 2014, 21, 1450019.	0.5	13
156	Comparison of Arsenic Adsorption on Goethite and Amorphous Ferric Oxyhydroxide in Water. Water, Air, and Soil Pollution, 2017, 228, 1.	1.1	13
157	Synthesis of montmorillonite-chitosan hollow and hierarchical mesoporous spheres with single-template layer-by-layer assembly. Journal of Materials Science and Technology, 2019, 35, 2325-2330.	5.6	13
158	Preparation of Carboxymethyl Cellulose-Based Hydrogel Supported by Two-Dimensional Montmorillonite Nanosheets for Methylene Blue Removal. Journal of Polymers and the Environment, 2021, 29, 3918-3931.	2.4	13
159	Rich Se nanoparticles modified cobalt carbonate hydroxide as an efficient electrocatalyst for boosted hydrogen evolution in alkaline conditions. Applied Surface Science, 2021, 565, 150505.	3.1	13
160	Adsorption of Zn(II) on graphene oxide prepared from lowâ€purity of amorphous graphite. Surface and Interface Analysis, 2017, 49, 398-404.	0.8	12
161	A novel dry vibrating HGMS separator for purification of potash feldspar ore. Separation Science and Technology, 2022, 57, 484-491.	1.3	12
162	Removal of Cu(II) from wastewater by using mechanochemically activated carbonate-based tailings through chemical precipitation. Environmental Science and Pollution Research, 2019, 26, 35198-35207.	2.7	11

#	Article	IF	CITATIONS
163	The Life Cycle of Water Used in Flotation: a Review. Mining, Metallurgy and Exploration, 2019, 36, 385-397.	0.4	11
164	First-principles study of X(O, Se, Te)-doped monolayer MoS2 for Hg0 adsorption. Physica E: Low-Dimensional Systems and Nanostructures, 2021, 127, 114504.	1.3	11
165	The Influence of Impurity Monovalent Cations Adsorption on Reconstructed Chalcopyrite (001)-S Surface in Leaching Process. Minerals (Basel, Switzerland), 2016, 6, 89.	0.8	10
166	A novel method for the quantitative determination of defects on graphene surfaces. Journal of Colloid and Interface Science, 2017, 499, 62-66.	5.0	10
167	Difference in the preparation of two-dimensional nanosheets of montmorillonite from different regions: Role of the layer charge density. Colloids and Surfaces A: Physicochemical and Engineering Aspects, 2021, 617, 126364.	2.3	10
168	Enhanced biodegradation of ciprofloxacin by enriched nitrifying sludge: assessment of removal pathways and microbial responses. Water Science and Technology, 2022, 85, 409-419.	1.2	10
169	Mechanism of the formation of micropores in the thermal decomposition of goethite to hematite. Surface and Interface Analysis, 2015, 47, 535-539.	0.8	9
170	Efficient removal of Hg2+ in aqueous solution with fishbone charcoal as adsorbent. Environmental Science and Pollution Research, 2018, 25, 7709-7718.	2.7	9
171	Laminar MoS2 membrane for high-efficient rejection of methyl orange from aqueous solution. Chemical Physics, 2020, 530, 110609.	0.9	9
172	Selective flotation separation of bastnaesite from dolomite using β-naphthyl sulfonate formaldehyde condensate as depressant: Experimental and calculational studies. Colloids and Surfaces A: Physicochemical and Engineering Aspects, 2022, 639, 128380.	2.3	9
173	Swelling Capacity of Montmorillonite in the Presence of Electrolytic Ions. Journal of Dispersion Science and Technology, 2016, 37, 380-385.	1.3	8
174	Preparation and Characterization of Nanoscale Zero-Valent Iron-Loaded Porous Sepiolite for Decolorizing Methylene Blue in Aqueous Solutions. Jom, 2017, 69, 699-703.	0.9	8
175	A case study on large-scale production for iron oxide pellets: Ezhou pelletization plant of the BAOWU. Mineral Processing and Extractive Metallurgy Review, 2018, 39, 211-215.	2.6	8
176	Floc-Flotation of Malachite Fines with an Octyl Hydroxamate and Kerosene Mixture. Minerals (Basel,) Tj ETQq0 0	0 rg.BT /Ov	verlock 10 Tf
177	Assessment of the structure, diversity, and composition of woody species of urban forests of Adama city, Central Ethiopia. Arboricultural Journal, 0, , 1-12.	0.3	8
178	Morphology of Hydrophobic Agglomerates of Molybdenite Fines in Aqueous Suspensions. Separation Science and Technology, 2015, 50, 1560-1564.	1.3	7
179	Stability of Na-montmorillonite suspension in the presence of different cations and valences. Journal of Dispersion Science and Technology, 2017, 38, 1035-1040.	1.3	7
180	Hydrophobic agglomeration kinetics of fine kaolinite particles in aqueous suspensions. Journal of Dispersion Science and Technology, 2017, 38, 1336-1341.	1.3	7

#	Article	IF	CITATIONS
181	Kinetic assessment of simultaneous removal of arsenite, chlorate and nitrate under autotrophic and mixotrophic conditions. Science of the Total Environment, 2018, 628-629, 85-93.	3.9	7
182	A Case Study on Large-scale Grate-kiln Production of Fluxed Iron Oxide Pellets: Zhanjiang Pelletizing Plant of BaoSteel. Mineral Processing and Extractive Metallurgy Review, 2019, 40, 123-128.	2.6	7
183	In-situ reduction of Au(S2O3)23â^' for efficient recovery of gold with magnetically separable shell-core structured MoS2@Fe3O4 composite. Hydrometallurgy, 2020, 198, 105514.	1.8	7
184	Synthesis of three-dimensional reduced graphene oxide aerogels as electrode material for supercapacitor application. Chemical Physics, 2021, 543, 111096.	0.9	7
185	Combined electrosorption and chemisorption of As(III) in aqueous solutions with manganese dioxide as the electrode. Environmental Technology and Innovation, 2021, 24, 101832.	3.0	7
186	INFLUENCE OF STICKY RICE AND ANIONIC POLYACRYLAMIDE ON THE CRYSTALLIZATION OF CALCIUM CARBONATE IN CHINESE ORGANIC SANHETU. Surface Review and Letters, 2015, 22, 1550073.	0.5	6
187	Delamination of Na-montmorillonite particles in aqueous solutions and isopropanol under shear forces. Journal of Dispersion Science and Technology, 2017, 38, 1117-1123.	1.3	6
188	Cr(VI) Removal from Water with Amorphous Graphite Concentrate Contaminated by Iron. Mineral Processing and Extractive Metallurgy Review, 2017, 38, 411-416.	2.6	6
189	Comparison Study on the Effect of Interlayer Hydration and Solvation on Montmorillonite Delamination. Jom, 2017, 69, 254-260.	0.9	6
190	Transforming Hematite into Magnetite Using Mechanochemical Approach as a Pretreatment of Oolitic Hematite. Mineral Processing and Extractive Metallurgy Review, 2017, 38, 24-29.	2.6	6
191	Comparison of Adsorption of Phenol O-O and N-O Chelating Collectors at the Malachite/Water Interface in Flotation. Minerals (Basel, Switzerland), 2017, 7, 20.	0.8	6
192	A Novel Model of Aggregate Gradation for Autoclaved Bricks from Tailings. Minerals (Basel,) Tj ETQq0 0 0 rgBT /0	Dverlgck 1	0 Tf 50 302 T
193	Reexamining the Adsorption of Octyl Hydroxamate on Malachite Surface: Forms of Molecules and Anions. Mineral Processing and Extractive Metallurgy Review, 2020, 41, 178-186.	2.6	6
194	Fabrication of self-supported Ni(OH)2@nickel nanowire coreshell arrays with enhanced electrochemical performance for supercapacitor applications. Scripta Materialia, 2020, 186, 79-83.	2.6	6
195	Highly stable MoS2@PDA composite for enhanced reduction of AuCl4â^'. Chemical Physics Letters, 2020, 747, 137350.	1.2	6
196	Liberation and Enrichment of Metallic Iron from Reductively Roasted Copper Slag. Jom, 2021, 73, 1013-1022.	0.9	6
197	MoS2 composite hydrogel supported by two-dimensional montmorillonite nanosheets for Pb2+ removal from water. Chemical Physics, 2022, 556, 111477.	0.9	6
198	Effect of exfoliation degree on the performance of montmorillonite nanosheets. Colloids and Surfaces A: Physicochemical and Engineering Aspects, 2022, 650, 129661.	2.3	6

#	Article	IF	CITATIONS
199	Decomposition characteristics of compound additive and effect of roasting atmosphere on vanadium extraction from stone coal. Asia-Pacific Journal of Chemical Engineering, 2017, 12, 374-380.	0.8	5
200	SYNTHESIS OF A COMPOSITE AEROGEL OF REDUCED GRAPHENE OXIDE SUPPORTED BY TWO-DIMENSIONAL MONTMORILLONITE NANOLAYERS FOR METHYLENE BLUE REMOVAL. Clays and Clay Minerals, 2021, 69, 746-758.	0.6	5
201	Synthetic Fe-rich nontronite as a novel activator of bisulfite for the efficient removal of tetracycline. Journal of Environmental Management, 2022, 302, 114002.	3.8	5
202	Roles of hydrocarbon chain-length in preparing graphene oxide from mildly-oxidized graphite with intercalating anionic aliphatic surfactants. RSC Advances, 2016, 6, 14859-14867.	1.7	4
203	Enhanced removal of fluoride from water through precise regulation of active aluminum phase using CaCO3. Environmental Science and Pollution Research, 2022, 29, 68555-68563.	2.7	4
204	Restraining Na-Montmorillonite Delamination in Water by Adsorption of Sodium Dodecyl Sulfate or Octadecyl Trimethyl Ammonium Chloride on the Edges. Minerals (Basel, Switzerland), 2016, 6, 87.	0.8	3
205	Effect of protonation and deprotonation reactions of clay on regulating pyrite flotation in the presence of clay. Colloids and Surfaces A: Physicochemical and Engineering Aspects, 2021, 609, 125654.	2.3	3
206	Investigation of Solid-State Carbothermal Reduction of Fayalite with and Without Added Metallic Iron. Jom, 2021, 73, 703-711.	0.9	3
207	A novel gasification exfoliation method of the preparation of anhydrous montmorillonite nanosheets for inhibiting restack problem suffering from dehydration. Applied Clay Science, 2022, 217, 106394.	2.6	3
208	Physical Disturbance Reduces Cyanobacterial Relative Abundance and Substrate Metabolism Potential of Biological Soil Crusts on a Gold Mine Tailing of Central China. Frontiers in Microbiology, 2022, 13, 811039.	1.5	3
209	ARSENIC REMOVAL FROM WATER BY ADSORPTION ON IRON-CONTAMINATED CRYPTOCRYSTALLINE GRAPHITE. Surface Review and Letters, 2017, 24, 1750099.	0.5	2
210	Synthesis of Fly Ash and Bentonite-Supported Zero-Valent Iron and Its Application for Removal of Toxic Cationic Dyes from Aqueous Solutions. Environmental Engineering Science, 2017, 34, 740-751.	0.8	2
211	Enhanced Production and Recovery of Orthophosphate from Wastewater Containing Phosphonate 1-Hydroxyethane-1,1-diphosphonic Acid through Combined Packed-Bed Ozonation and Adsorption. ACS Sustainable Chemistry and Engineering, 2021, 9, 16946-16955.	3.2	2
212	ELECTROKINETIC CHARACTERISTICS OF CALCINED KAOLINITE IN AQUEOUS ELECTROLYTIC SOLUTIONS. Surface Review and Letters, 2015, 22, 1550041.	0.5	1
213	Enhanced adsorption performance of the graphene oxide with metallic ion impurities by elution. Surface and Interface Analysis, 2017, 49, 728-734.	0.8	1
214	Recovery of Au(CN) ₂ ^{â^'} by adsorption using reduced graphene oxide/ascorbic acid hydrogel. Mineral Processing and Extractive Metallurgy: Transactions of the Institute of Mining and Metallurgy, 2018, 127, 140-145.	0.1	1
215	Effects of Rectifying Bundles on Desliming Ponds. International Journal of Coal Preparation and Utilization, 2021, 41, 30-39.	1.2	1
216	Construction of MoS ₂ @Activated Alumina Beads as Catalysts for Rapid Gold Recovery from Au(S ₂ O ₃) ₂ ^{3–} Solution. Langmuir, 2022, 38, 8054-8064.	1.6	1

#	Article	IF	CITATIONS
217	The reduction mechanism of HAuCl4 on the surface of edge-rich molybdenum disulfide. Surfaces and Interfaces, 2022, 33, 102199.	1.5	1
218	Rupture Force of Magnetite Chain in a Uniform Magnetic Field. Separation Science and Technology, 2014, 49, 2437-2439.	1.3	0